Effect of Diluent on Poly(ethylene-*co*-vinyl alcohol) Hollow-Fiber Membrane Formation via Thermally Induced Phase Separation

Mengxian Shang,[1] Hideto Matsuyama,[1] Masaaki Teramoto,[1] Junpei Okuno,[1] Douglas R. Lloyd,[2] Noboru Kubota[3]

[1]*Department of Chemistry and Materials Technology, Kyoto Institute of Technology, Matsugasaki, Sakyo-ku, Kyoto 606-8585, Japan*
[2]*Department of Chemical Engineering, University of Texas at Austin, Austin, Texas 78712*
[3]*Asahi Chemical Industry Co., Ltd., 2-1 Samejima, Fuji, Shizuoka 416-8501, Japan*

Received 27 June 2003; accepted 15 July 2004
DOI 10.1002/app.21193
Published online in Wiley InterScience (www.interscience.wiley.com).

ABSTRACT: Poly(ethylene-*co*-vinyl alcohol) hollow-fiber membranes with a 44 mol % ethylene content were prepared by thermally induced phase separation. A mixture of 1,3-propanediol and glycerol was used as the diluent. The effects of the ratio of 1,3-propanediol to glycerol in the diluent mixture on the phase diagram, membrane structure, and membrane performance were investigated. As the ratio increased, the cloud point shifted to lower temperatures, and the membrane structure changed from a cellular structure due to liquid–liquid phase separation to a particulate structure due to polymer crystallization. Better pore connectivity was obtained in the hollow-fiber membrane when the ratio of 1,3-propanediol to glycerol was 50:50, and the membrane showed about 100 times higher water permeability than the membrane prepared with pure glycerol. For the prepared hollow-fiber membrane, the solute 20 nm in diameter was almost rejected. © 2004 Wiley Periodicals, Inc. J Appl Polym Sci 95: 219–225, 2005

Key words: phase separation; hollow fibers; membranes

INTRODUCTION

Thermally induced phase separation (TIPS) in polymer solutions is one of the most versatile and widely used methods used to produce a variety of microporous membranes.[1,2] In the TIPS process, a homogeneous solution needs to be formed by the dissolution of a polymer in a diluent at a high temperature, and phase separation is induced by the cooling of the polymer solution. Thus, the compatibility between the polymer and diluent is one of the key factors affecting morphology. In a large number of studies on TIPS, polyolefin has been used as the polymer material to prepare microporous membranes.[3–9] Poly(ethylene-*co*-vinyl alcohol) (EVOH) crystalline copolymer is also a candidate polymer for membrane preparation via the TIPS process because EVOH has a hydrophilic vinyl alcohol segment and it can prevent membrane fouling in the membrane separation application. Young and his coworkers published a series of articles on the immersion precipitation technique for the preparation of EVOH membranes.[10–14] Highly porous and crystalline membranes were obtained, and membranes with leafy morphology were created through liquid–liquid (L–L) phase separation, which was followed by crystallization.

In our previous studies, EVOH membranes were prepared via the TIPS process.[15–17] Both 1,3-propanediol and 1,3-butanediol were used as diluents in our serial studies on the preparation of EVOH membranes via TIPS. Those results showed that the membrane performances were influenced by the kinds of diluents used in the TIPS process. In a EVOH–glycerol system, the structural variation of EVOH membranes was investigated in terms of polymer–diluent thermodynamics[18] and polymer crystallization kinetics.[19]

Compared to flat membranes, hollow-fiber membranes have much wider applications at the commercial scale because they enable a higher membrane area per unit membrane module volume.[20] Sun et al. prepared a high-density polyethylene hollow-fiber membrane by polymer crystallization via the TIPS process.[21,22] In our laboratory, polyethylene and EVOH hollow-fiber membranes were prepared by L–L phase separation in the TIPS process.[23,24] The effects of polymer molecular weight, polymer density, air gap distance, water bath temperature, and the kind of diluent on membrane structure and performance were investigated extensively.

In membrane preparation via TIPS, the selection of diluent is quite important because it effects not only

Correspondence to: H. Matsuyama (matuyama@chem.kit.ac.jp).

the phase diagram but also the kinetics of pore growth. The role of the diluent in TIPS membranes was examined for solid–liquid phase separation systems in terms of the diluent mobility and crystallization temperature (T_c).[25] Vadalia et al. prepared microporous membranes by TIPS of a ternary solution of high-density polyethylene, ditrydecylphthalate, and hexadecane.[26] In their work, the solvent mixture was considered as one component to show the effect of the interaction parameter on the phase diagram. The membrane morphology was controlled successfully by variation of the composition of the solvent pair while the cooling conditions were kept constant.

In this study, 1,3-propanediol, glycerol, and their mixture were used as the diluents in the preparation of EVOH hollow-fiber membranes. The objective of this study was to demonstrate the effect of the diluent on hollow-fiber membrane formation and membrane performance.

EXPERIMENTAL

Materials

EVOH with a 44 mol % ethylene content (EVOH44) was supplied from Nihon Gohsei Chemical Industry Co., Ltd. (Osaka, Japan). Glycerol and 1,3-propanediol (Wako Pure Chemical Industries, Ltd., Kyoto, Japan) were used as diluents. All of the chemicals were used without further purification.

Determination of the phase diagram

The cloud point (T_{cloud}) and crystallization temperature (T_c) were measured by a method used previously.[19] A homogeneous polymer–diluent sample (the polymer concentration was 30 wt %) was placed between a pair of microscope cover slips. A 100 μm thick Teflon film with a square opening was inserted between the cover slips. The sample was heated on an LK-600 PH hot stage (Linkam, Surrey, UK) to 200°C for 1 min and cooled to 25°C at a controlled rate of 1°C/min. Subsequently, T_{cloud} was determined visually by notation of the appearance of turbidity under a BX50 optical microscope (Olympus, Tokyo).

A PerkinElmer DSC-7 was used to determine the dynamic T_c. The solid sample was sealed in an aluminum differential scanning calorimetry pan, melted at 200°C for 3 min, and then cooled at 10°C/min to 50°C. The onset of the exothermic peak during the cooling was taken as the T_c.

Light-scattering measurement

The light-scattering measurement was carried out to clarify the phase separation kinetics in the polymer solution with a polymer dynamics analyzer (Otsuka Electronics Co., DYNA-1100T, Hirakata, Japan).[19] Solid samples prepared with several diluents and with different ratios of 1,3-propanediol to glycerol were sealed with two cover slips and placed on the hot stage located between a He–Ne laser and a detector. The hot stage was set to 200°C for melting the sample, and then the sample was cooled to 40°C at a rate at 130°C/min. The structure growth behavior during cooling was measured at a time interval of 0.1 s.

Flat membrane preparation

A homogeneous polymer–diluent sample with a polymer concentration of 30 wt % was placed between a pair of microscope cover slips. The thickness of the sample was adjusted at 100 μm by insertion of the Teflon film between the slips. The sample was heated at 200°C for 1 min on the hot stage and cooled to 25°C at a cooling rate of 10°C/min. The diluent in the flat membrane was extracted by immersion in water.

Hollow-fiber membrane preparation

Hollow-fiber membranes were prepared by a batch-type extruder (Imoto Co. BA-0, Kyoto, Japan).[23,24] EVOH44 (25 wt %) solutions with several weight ratios of 1,3-propanediol to glycerol (0:100, 50:50, and 100:0) were fed to the vessel and mixed at 200°C for 15 min under a nitrogen atmosphere. After it was held at this high temperature for 1 h, the homogeneous polymer solution was fed to a spinneret with an outer diameter of 1.58 mm and an inner diameter of 0.83 mm by a gear pump under a nitrogen pressure of 0.15 MPa. The diluent was introduced into the inner orifice of the spinneret to make the lumen of the hollow fiber to prevent diluent evaporation. The polymer solution extruded from the spinneret was put in a 40°C water bath to induce phase separation, and it was wound on a take-up winder to obtain the hollow fibers. The diluent remaining in the hollow-fiber membranes was extracted by water. In the spinning process, the air gap distance from the spinneret to the top level of water bath was 5 mm; the extrusion rate of the polymer solution and the bore diluent flow rate were almost fixed at 0.12 and 0.27 m/s, respectively; the take-up speed was controlled at 0.19, 0.32, and 0.38 m/s, respectively.

Characterization of the hollow-fiber membranes

After the diluents were replaced with water, the flat and hollow-fiber membranes were freeze-dried. The obtained dry membranes were fractured in liquid nitrogen and treated with Au/Pd sputtering. The cross-sections and surfaces of the membranes were examined with an S-800 scanning electron microscope (Hi-

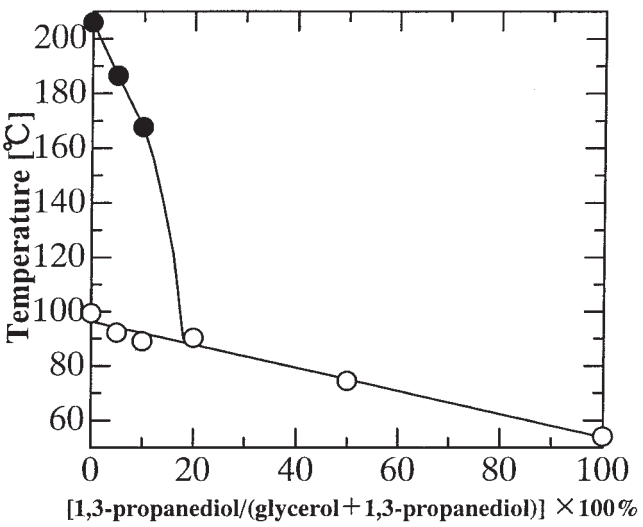

Figure 1 Effect of 1,3-propanediol composition in the diluent on the phase diagram (polymer concentration: 30 wt %): (●) T_{cloud} and (○) T_c.

tachi Co., Tokyo) with an accelerating voltage of 20 kV.

A water permeation test and filtration experiment for the hollow-fiber membranes were performed by a method described previously.[23,24] In the water permeation test, pure water was forced to permeate from the inside to the outside of the hollow-fiber membrane, and the water permeability was calculated on the basis of the inner surface area of the hollow-fiber membrane. In the filtration experiment, three kinds of polystyrene latex particles (100, 50, and 20 nm) were used as the different sizes of solutes. The solute concentrations in the filtrate (C_0) and in the feed solution (C_f) were measured with an U-200 ultraviolet spectrophotometer (Hitachi) under the wavelength of 385 nm.

RESULTS AND DISCUSSION

Phase diagram

Figure 1 shows the phase diagram of 30 wt % EVOH44 samples prepared with several diluents with different ratios of 1,3-propanediol to glycerol. Both T_{cloud} and T_c decreased with increasing 1,3-propanediol content in the diluents. When the 1,3-propanediol ratio in the diluent was over 20:80, no L–L phase separation was observed, and only polymer crystallization was obtained. The comparison of solubility parameters between polymer and diluent is a useful way to interpret the phase diagram.[15,27] The solubility parameters of the polymer and diluents involved in this system are listed in Table I. The difference of the solubility parameters between EVOH44 and 1,3-propanediol was much smaller than that between EVOH44 and glycerol, which means that 1,3-propanediol was more compatible with EVOH44. Therefore, T_{cloud} decreased with increasing 1,3-propanediol content. Thus, the phase diagram was definitely influenced by the variation of the mixing ratio in the diluent mixture.

Effect of the diluent on the flat membrane structure

Figure 2 shows the cross-sectional structures of flat membranes prepared with several diluents with various ratios of 1,3-propanediol to glycerol. Hereafter, the diluents with ratios of 1,3-propanediol to glycerol of 0:100, 20:80, 50:50, and 100:0 are abbreviated as 0:100, 20:80, 50:50, and 100:0 diluent, respectively. As shown in Figure 1, the binodal point was much higher than its T_c in the 0:100 diluent system (the pure glycerol system). Therefore, the L–L phase separation proceeded well with cooling until it was solidified by the polymer crystallization, and only cellular pores were formed in this membrane, as shown in Figure 2(a). In the 20:80 diluent system, spherulites due to both polymer crystallization and cellular pores were obtained, as shown in Figure 2(b). This was due to the sequential occurrence of L–L TIPS just after polymer crystallization. However, only the spherulites were observed in both the 50:50 and 100:00 diluent systems, as shown in Figure 2(c), (d). Because the polymer crystallization occurred before the L–L phase separation in these two systems and because their T_c values were very low, there was no allowance for the occurrence of L–L phase separation until the structure was solidified. Thus, the membrane structure formed by TIPS could be controlled by variation of the kind of diluent.

Kinetic study

Light scattering of the 25 wt % polymer solutions was measured during cooling. Figure 3 shows the light-scattering results for the 20:80 diluent system. The scattered light intensity (I_s) showed a maximum in the plot of I_s versus the scattered angle (θ), indicating that phase separation was followed by spinodal decomposition (SD) rather than nucleation and growth.[28] Moreover, the angle at which I_s showed the maximum did not shift to the smaller angle region, which indicated that the structure formed by the phase separation hardly grew.

TABLE I
Solubility Parameters for the Substances Used in This Study

Substance	Solubility parameter ($MPa^{1/2}$)
EVOH44	21.4[18]
1,3-Propanediol	24.0[15]
Glycerol	33.8[18]

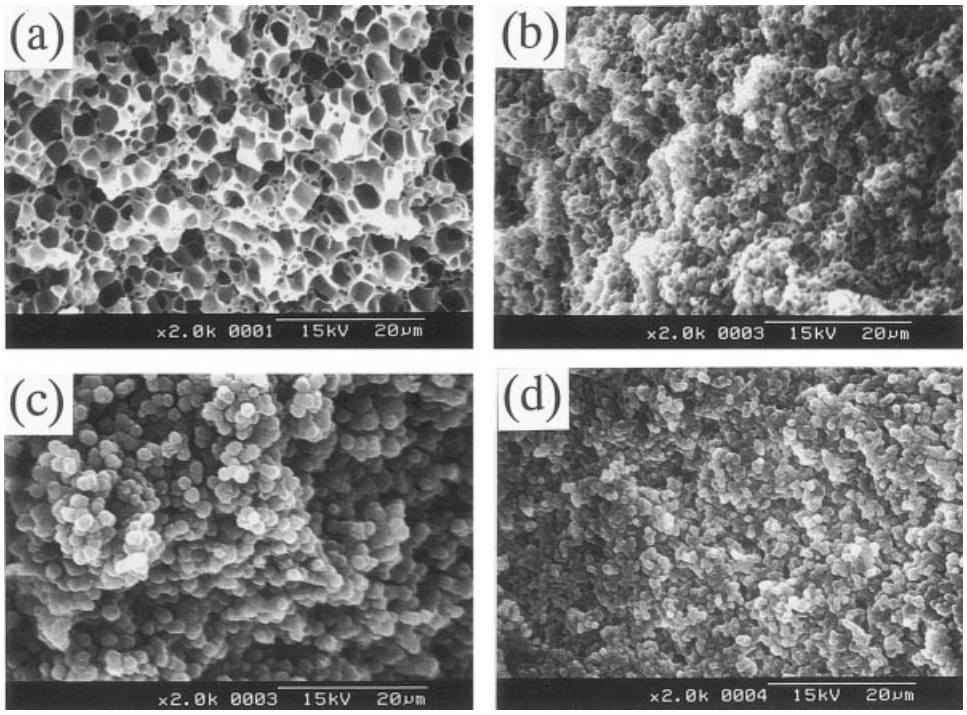

Figure 2 Scanning electron microscopy images of cross-sections of 30 wt % EVOH44 flat membranes (cooling rate: 10°C/min): (a) 0:100, (b) 20:80, (c) 50:50, and (d) 100:0 diluent systems.

The interphase periodic distance (Λ) formed by SD can be related to θ, where I_s shows a maximum, by the following equation:

$$\Lambda = \frac{\lambda_0}{2n_0 \sin\left(\frac{\theta}{2}\right)} \tag{1}$$

where n_0 is the reflection coefficient and λ_0 is the wavelength *in vacuo* (633 nm). The comparison of the time courses of Λ in the 0:100, 20:80, and 50:50 diluent systems are shown in Figure 4. In the 0:100 diluent system, the structure grew fast, whereas in both the 20:80 and 50:50 diluent systems, the structure hardly changed with time. The final structure size decreased in the following order: 0:100, 20:80, and 50:50 diluent systems. This kinetic result can be understood based on the phase diagram shown in Figure 1. Although the polymer concentration of the sample used in the light-scattering experiment was somewhat lower than that used in Figure 1, the fundamental behavior of the phase diagram was the same in both cases. In the 0:100 diluent system, the binodal temperature was much higher than T_c, the L–L phase separation occurred

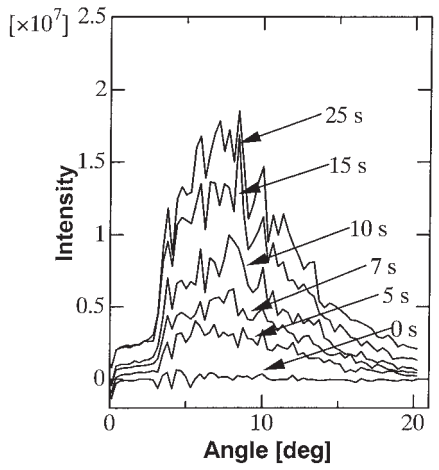

Figure 3 Light-scattering results in the 20:80 diluent system (polymer concentration: 25 wt %, cooling rate: 130°C/min).

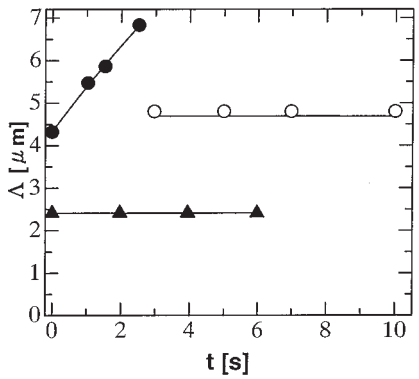

Figure 4 Time (t) course of Λ: (●) 0:100, (○) 20:80, and (▲) 50:50 diluent systems.

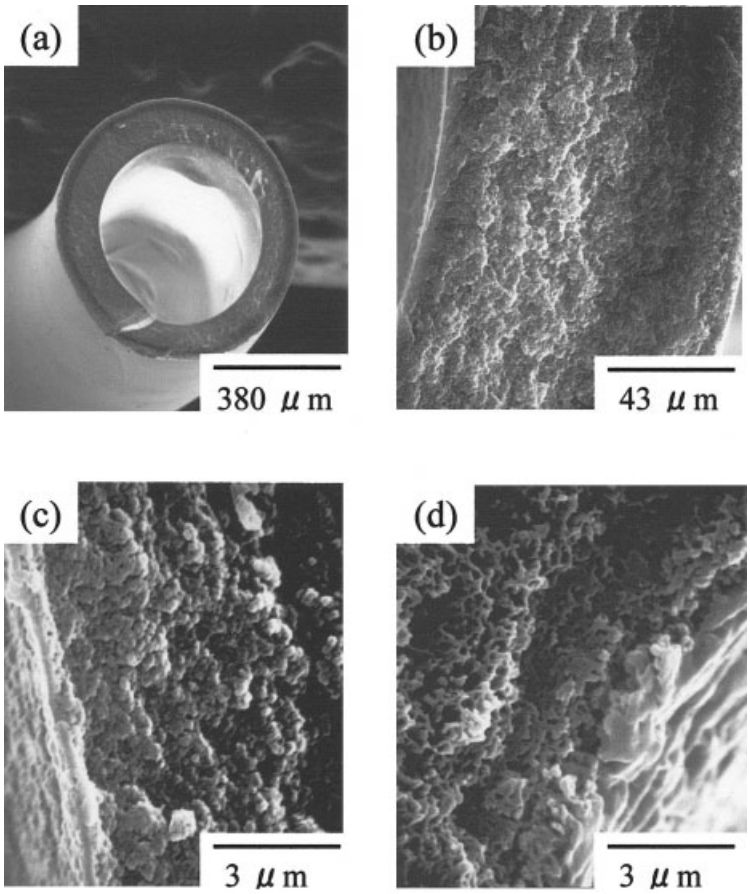

Figure 5 Scanning electron microscopy images of the hollow-fiber membrane of the 100:0 diluent system (take-up speed: 0.38 m/s): (a) whole cross-section, (b) enlarged cross-section, (c) cross-section near the inner surface, and (d) cross-section near the outer surface.

first, and it thermodynamically allowed the droplet to grow with a sufficient time, as reported in our previous article.[29] Thus, Λ could grow well, as shown in Figure 4. When the 1,3-propanediol ratio in the diluent was increased, T_{cloud} decreased drastically, as shown in Figure 1. In both the 20:80 and 50:50 diluent systems, the T_{cloud} values were below T_c. Thus, we deduced that the phase separation structure was solidified shortly because of the occurrence of polymer crystallization. This is the reason that Λ in the 20:80 and 50:50 diluent systems remained unchanged in this experimental time scale. As the 1,3-propanediol ratio in the diluent increased, T_{cloud} decreased, which meant that the time interval for the structure growth became shorter. Thus, the final size decreased with increasing 1,3-propanediol ratio.

Structure of hollow-fiber membrane

Figure 5 shows a hollow-fiber membrane structure prepared in the 100:0 diluent system at a take-up speed of 0.38 m/s. The whole cross-sectional structure and its enlarged structure are shown in Figure 5(a,b). Figure 5(c,d) shows the cross-sectional structures near the inner and outer surfaces, respectively. The outer diameter, inner diameter, and membrane thickness were 733, 459, and 137 μm, respectively. The internal structure near the outer surface was significantly different from that near the inner surface. Only the spherulites were formed near the inner surface, as shown in Figure 5(c), and both spherulites and cellular pores were formed near the outer surface, as shown in Figure 5(d). On the basis of the phase diagram shown in Figure 1, in the 100:0 diluent system, we deduced that polymer crystallization occurred before the L–L phase separation, and T_c was as low as 60°C. Therefore, we predicted that the polymer crystallized without the occurrence of L–L phase separation and the membrane structure solidified by crystallization. Thus, it is reasonable that only the particulate structure was observed near the inner surface. However, the cellular pores coexisted with the spherulites near the outer surface. As reported in our previous article,[29] after the membrane was immersed into a water bath during spinning, water penetrated into the membrane from the outer surface due to the good compatibility

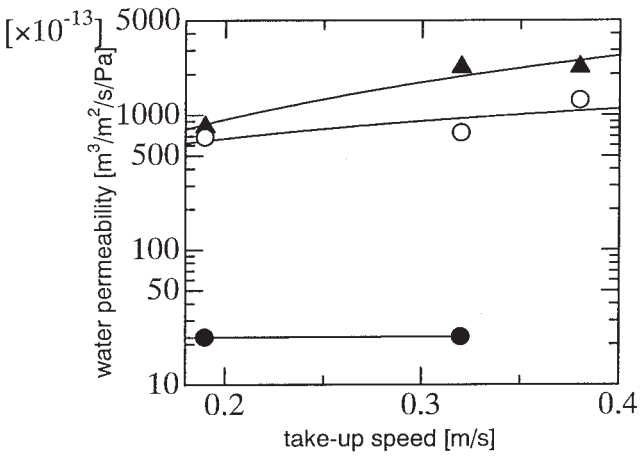

Figure 6 Effect of the diluent on the water permeability of the hollow-fiber membranes: (●) 0:100, (▲) 50:50, and (○) 100:0 diluent systems.

between the diluent and water. Because water was the nonsolvent for EVOH44, T_{cloud} shifted to the higher temperature due to the penetration of water. Therefore, L–L phase separation was likely to occur, which resulted in the coexistence of spherulites and cellular pores near the outer surface.

Water permeability

The effect of the diluent on water permeability is shown in Figure 6. The membranes prepared in the 50:50 and 100:0 diluent systems showed about 100 times higher permeabilities than the membrane with pure glycerol (the 0:100 diluent system). Thus, the addition of 1,3-propanediol to glycerol is one useful way to enhance membrane performance. This result can be discussed in connection with the cross-sectional structures near the outer surface of the membranes shown in Figure 7. The pore size near the outer surface increased in the order 100:0, 50:50, and 0:100 diluent systems. This tendency agreed with the light-scattering results described in Figure 4. For the membrane prepared in the 0:100 diluent system, as reported in our previous article,[29] the longer growth time of L–L phase separation led to isolated structure formation and poor pore connectivity. This was the reason for the lowest permeability shown in Figure 6, although the pore size was larger. In comparison to this membrane, the pore connectivity in the membrane prepared in the 50:50 diluent system [Fig. 7(b)] was greatly improved due to the short growth time of droplets formed by L–L phase separation because T_{cloud} shifted to a lower temperature with the addition of 1,3-propandiol, as shown in Figure 1. Therefore, the water permeability of the membrane became larger. The pore size near the outer surface of the membrane prepared in the 50:50 diluent system [Fig. 7(b)] was larger than that in 100:0 diluent system [Fig. 7(c)]. Thus, the former membrane showed a higher water permeability.

Solute rejection

The solute rejection coefficient (R) is defined as

$$R = 1 - C_f/C_0 \tag{2}$$

The obtained results for two membranes prepared in the 50:50 and 100:0 diluent systems are illustrated in Figure 8. Both two membranes showed high rejection coefficients, even for polystyrene particles with a diameter of 20 nm.

CONCLUSIONS

The phase diagram of EVOH44 in several diluents of a mixture of 1,3-propanediol and glycerol was clarified. T_{cloud} and T_c decreased as the ratio of 1,3-propanediol to glycerol in the diluent increased.

The phase separation kinetics were examined by light-scattering measurements. We confirmed that

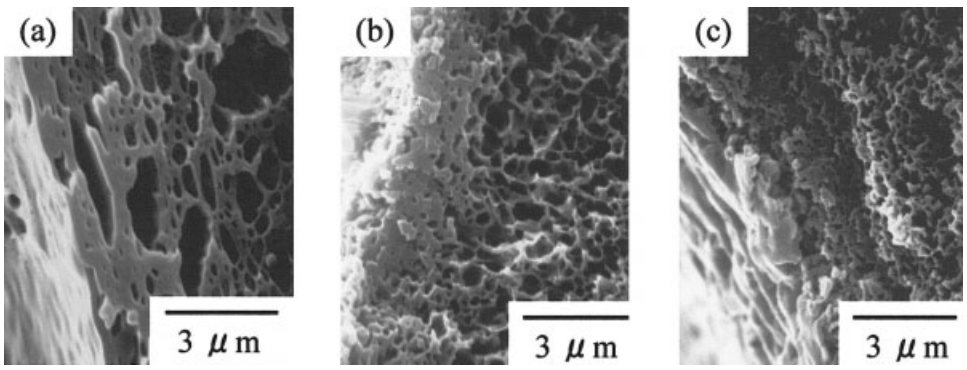

Figure 7 Cross-sectional structures near the outer surface of the hollow-fiber membranes: (a) 0:100, (b) 50:50, and (c) 100:0 diluent systems.

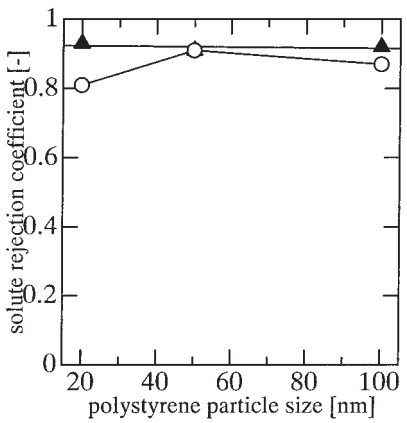

Figure 8 *R* values of the hollow-fiber membrane: (▲) 50:50 and (○) 100:0 diluent systems.

the phase separation was followed by SD. A faster growth rate and larger structure were obtained in the 0:100 pure glycerol system due to a higher T_{cloud}. However, in the 50:50 and 100:0 diluent systems, the structures hardly grew in the experimental timescale.

Microporous hollow-fiber membranes were prepared from EVOH44 solutions with various diluents via a TIPS process. For the 100:0 (pure 1,3-propanediol) system, cellular pores due to L–L phase separation were formed near the outer surface, whereas the particulate structure due to polymer crystallization was formed near the inner surface. Water could penetrate into the membrane from the outer surface during the spinning process, which led to a shift in T_{cloud} to a higher temperature, and L–L phase separation was likely to occur. Thus, cellular pores were formed near the outer surface. The addition of 1,3-propanediol to the diluent was quite effective in enhancing the water permeability of the membrane. The membrane prepared in the 50:50 diluent system showed about 100 times higher permeability than that in pure glycerol system. The prepared hollow-fiber membrane had high solute rejection properties. The solute 20 nm in diameter was almost rejected.

References

1. Castro, A. J. U.S. Pat. 4,247,498 (1981).
2. Lloyd, D. R. Materials Science of Synthetic Membranes; ACS Symp Series 269; American Chemical Society: Washington, DC, 1985; p 1.
3. Lloyd, D. R.; Kinzer, K. E.; Tseng, H. S. J Membr Sci 1990, 52, 239.
4. Lloyd, D. R.; Kim, S.-S.; Kinzer, K. E. J Membr Sci 1991, 64, 1.
5. Kim, S.-S.; Lloyd, D. R. J Membr Sci 1991, 64, 13.
6. Matsuyama, H.; Berghmans, S.; Lloyd, D. R. Polymer 1999, 40, 2289.
7. Matsuyama, H.; Yuasa, M.; Kitamura, Y.; Teramoto, M.; Lloyd, D. R. J Membr Sci 2000, 179, 91.
8. Matsuyama, H.; Okafuji, H.; Maki, T.; Teramoto, M.; Tsujioka, N. J Appl Polym Sci 2002, 84, 1701.
9. Matsuyama, H.; Maki, T.; Teramoto, M.; Asano, K. J Membr Sci 2002, 204, 323.
10. Young, T. H.; Huang, Y. H.; Chen, L. Y. J Membr Sci 2000, 164, 111.
11. Young, T. H.; Huang, Y. H.; Huang, Y. S. J Membr Sci 2000, 171, 197.
12. Cheng, L. P.; Young, T. H.; Chung, Y. W.; Chen, L. Y. Polymer 2001, 42, 443.
13. Young, T. H.; Cheng, L. P.; Hsieh, C. C.; Chen, L. W. Macromolcules 1998, 31, 1229.
14. Young, T. H.; Hsieh, C. C.; Chen, L. Y.; Huang, Y. S. J Membr Sci 1999, 159, 21.
15. Matsuyama, H.; Iwatani, T.; Kitamura, Y.; Teramoto, M. J Appl Polym Sci 2001, 79, 2449.
16. Matsuyama, H.; Iwatani, T.; Kitamura, Y.; Teramoto, M. J Appl Polym Sci 2001, 79, 2456.
17. Matsuyama, H.; Kobayashi, K.; Maki, T.; Teramoto, M. J Appl Polym Sci 2001, 82, 2583.
18. Shang, M. X.; Matsuyama, H.; Maki, T.; Teramoto, M.; Lloyd, D. R. J Appl Polym Sci 2003, 87, 853.
19. Shang, M. X.; Matsuyama, H.; Maki, T.; Teramoto, M.; Lloyd, D. R. J Polym Sci Part B: Polym Phys 2003, 41, 194.
20. Zeman, L. J.; Zydney, A. L. Microfiltration and Ultrafiltration; Marcel Dekker: New York, 1996.
21. Sun, H.; Rhee, K. B.; Kitano, T.; Mah, S. I. J Appl Polym Sci 1999, 73, 2135.
22. Sun, H.; Rhee, K. B.; Kitano, T.; Mah, S. I. J Appl Polym Sci 1999, 75, 1235.
23. Matsuyama, H.; Okafuji, H.; Maki, T.; Teramoto, M.; Kubota, N. J Membr Sci 2003, 223, 119.
24. Matsuyama, H.; Hayashi, K.; Maki, T.; Teramoto, M.; Kubota, N. J Appl Polym Sci 2004, 93, 471.
25. Kim, S. S.; Lim, B. A.; Alwattari, A. A.; Wang, Y. F.; Lloyd, D. R. J Membr Sci 1991, 64 41.
26. Vadalia, H. C.; Lee, H. K.; Myerson, A. S.; Levon, K. J Membr Sci 1994, 89, 37.
27. Liu, B.; Du, Q.-G.; Yang, Y.-L. J Membr Sci 2000, 180, 81.
28. Nunes, S. P.; Inoue, T. J Membr Sci 1996, 111, 93.
29. Shang, M. X.; Matsuyama, H.; Maki, T.; Teramoto, M.; Lloyd, D. R.; Kubota, N. Polymer 2003, 44, 7441.